CHAPTER II

DESCRIPTION OF THE EXPERIMENTAL TECHNIQUES

2.1 Introduction

The design of the experimental set up for high pressure investigation of liquid crystals presents certain problems which are not normally encountered in the study of the solid state, e.g., containment of the liquid crystalline substance, low heat of transition, chemical reactivity with the material of the container etc. In addition most liquid and solid pressure transmitting media contaminate the liquid crystalline material, and even a minute contamination results in a drastic reduction of the transition temperature. If gas is used as pressure transmitting medium it will dissolve in the liquid crystalline sample and no meaningful measurements can be made.

Taking all these factors into consideration the author has designed and fabricated a high pressure optical cell. Most of the results presented in this thesis have been obtained using this cell. The author has also carried out Xray and dielectric studies to supplement the results obtained from high pressure experiments. The description of the different types of apparatus forms the subject matter of this chapter.

2.2 High **Pressure Optical Cell**

Optical transmission technique was the earliest method used to detect phase transitions at high pressure.[1,2] More recently, this technique has been used with considerable success, by Keyes et al,[3] Cladis et al[4] and Kalkura et al.[5] All these studies have been conducted using direct pressure transmitting cells which have been designed for forward scattering experiments. Although one such cell did exist in the laboratory,[5] the author felt the need to modify this cell in view of two requirements:

1. to construct a cell which can be used both for light scattering and optical microscopy experiments - a need which becomes particularly important in identifying pressure induced phases and
2. to design a cell which is usable even for very small quantities of the sample (< 5mg).

In this section a detailed description of the cell covering the design as well as the constructional aspects will be given.

2.2.1 Description of the Cell

A schematic diagram of the high pressure optical cell is given in fig. 2.1. All the components of the cell were machined out of a low alloy hardenable steel, viz., *EN-24* (equivalent to AISI 4130) which has 0.4% carbon, 0.2% silicon and 0.55% nickel. This steel has the advantage that it can be hardened

Figure 2.1

HIGH PRESSURE OPTICAL CELL

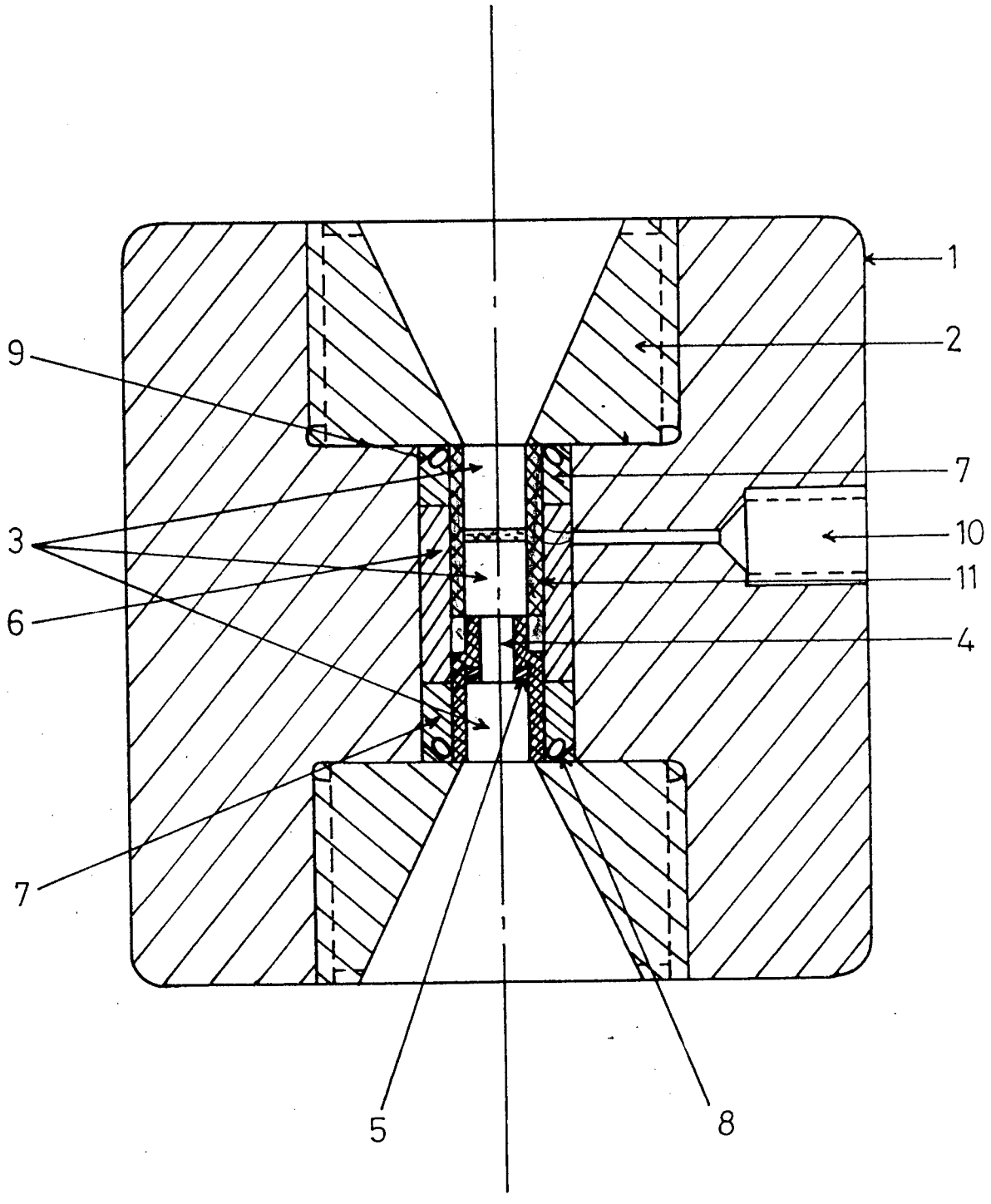

1. CELL BODY 2, STEEL PLUG 3, SAPPHIRE CYLINDERS

4, GLASS ROD 5, WASHER AND SPRING 6, CENTRE SPACER

7, OUTER SPACER 8, '0' RING 9. ANTIEXTRUSION RING

10. HIGH PRESSURE CONNECTION 11. FLURAN TUBE,

to great strengths by means of martensitic transformation. The alloying elements increase the hardenability of the material and in addition, also contribute with solid-solution strengthening. The different parts of the cell were machined and heat treated to hardnesses ranging from 40 to 55 RC depending on the component and its location in the cell.

The body of the cell (fig.2.2) has threaded openings on both sides into which the two plugs (see fig. 2.1) with exactly matching threads can be fitted. On the outside, the plugs have a large tapered opening (70° outside taper) which facilitates a wide viewing angle without affecting the strength of the plug. .On the inside, the plugs have a small protrusion which are made optically flat by handlapping. These plugs keep the sample assembly in position. The central hole of the upper plug is sealed by an optically polished sapphire rod which also forms a part of the sample assembly. The hole in the cell body for the pressure connection consists of two stages: a smaller hole which extends from the interior of the body to about two-thirds of the thickness and joins a larger hole bored from outside.

2.2.2 Sample Chamber

In order to develop high pressure in the small central sample chamber, it is essential to have a tight seal along both boundaries of the plugs: one for the central hole and the other along the circular boundary of the chamber against the plug. The reason for the latter is that the threadsof the plug alone are not enough to hold the plug tightly against the main body of the

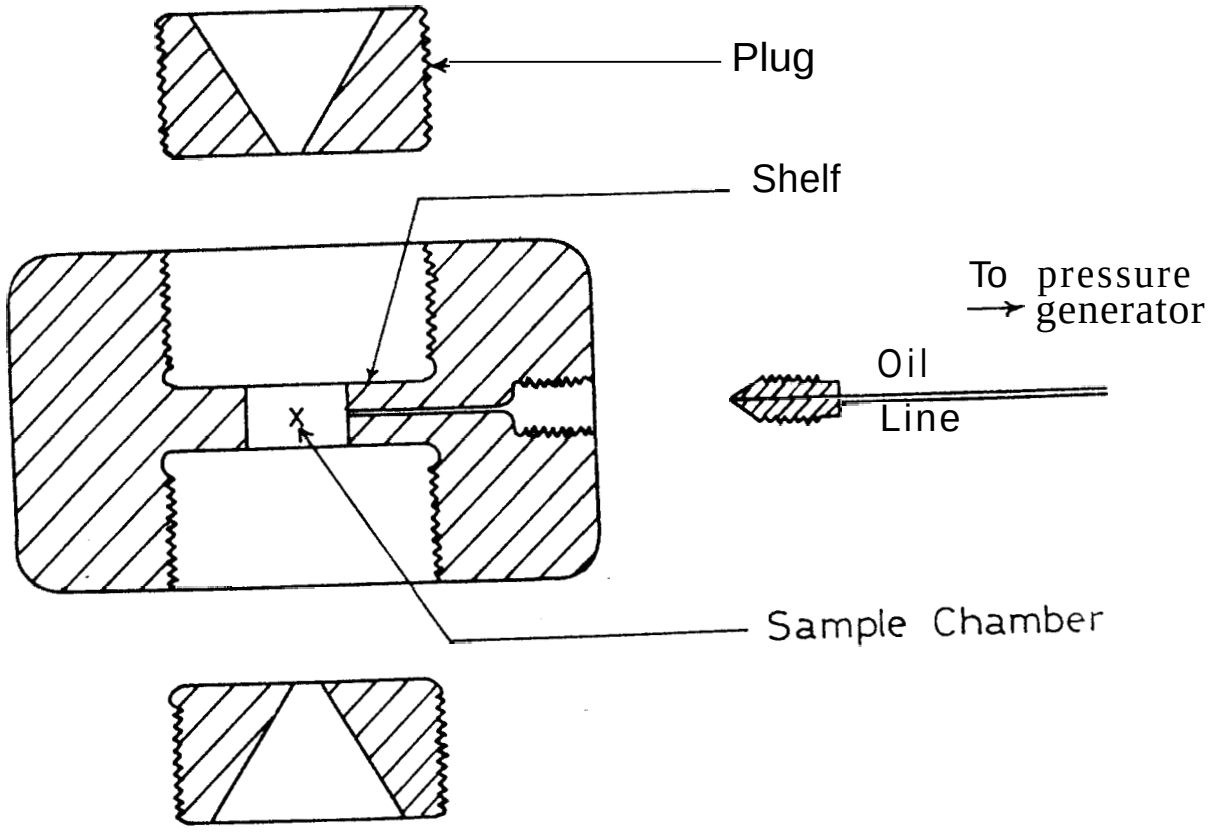

Figure 2.2 Schematic diagram of the basic parts of the high pressure cell

cell. A thin clearance between the plug and the sample chamber caused by a slight lifting of the plug by high pressure leads to a leak of the oil to the outside. This leak is avoided by placing around the junction a neoprene 'O' ring in conjunction with an anti-extrusion ring. The seal at the central hole of the plug is made with optically polished sapphire windows and a small washer made of thin aluminium foil- the washer to fill any crevices on the surface of the plug. The sapphire windows as well as the 'O' ring are held in position initially by the outer spacer.

Encapsulation of the Sample

As mentioned earlier, liquid crystals interact with the pressure transmitting fluid. It is therefore necessary to isolate the sample from the pressure transmitting medium. This is achieved by using a fluran tubing. Fluran, an elastomer material does not react with liquid crystals and at the same time transmits pressure exceedingly well. It can also withstand temperatures upto about 270°C. The sample assembly is schematically represented in fig. 2.3. The sample is sandwiched between two sapphire rods which fit snugly inside the fluran tube. An effective seal is realised by tightly wrapping a thin steel wire around the tubing on the sapphire windows. The innner spacer (low pressure sealer), washer and the spring (see fig. 2.1) centre the bottom sapphire (which is free as it is not used to seal the cap) of the sample assembly and keep it under a light tension. The third sapphire which is completely isolated from the sample assembly seals the bottom end of the pressure cell. The space between this third sapphire and the bottom sapphire of the sample assem-

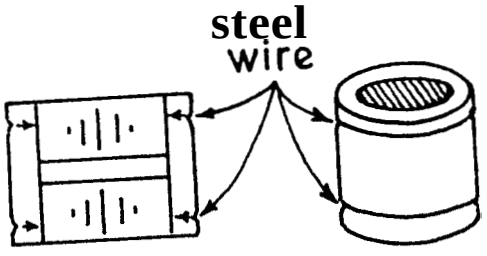

Figure 2.3 Sample assembly

bly is occupied by a glass rod reducing thereby the amount of oil between these two sapphires which otherwise would have decreased the intensity of the transmitted light. It must also be mentioned that all the three sapphire rods are specially cut such that the C-axis is perpendicular to the faces.

2.2.3 Description of the Heatinq and Coolinq Systems

Most of the experiments conducted by the author required quite high temperatures (about 200°C) and hence it was necesssary to have a heating system which can rise the temperature of the entire pressure cell. Fig. 2.4 shows the schematic diagram of the heater and the cooler assemblies. The heating system is made of an aluminum cylinder whose internal diameter is such that the pressure cell could be push-fitted into it. Thus it also acts as a binding ring for the pressure cell. Nichrorne tape was wound on mica sheets-which served as an electrical insulator - and the mica strips in turn were wrapped around the inside wall of the aluminum cylinder. The effective heatinq capacity was about 200 watts. A radial hole was made through the aluminium cylinder to facilitate the taking out of the pressure tubings from the pressure cell to the outside. A Chromel-Alumel thermocouple sheathed in a ceramic tube was used to measure the temperature sensed by the sample. The thermocouple is introduced through a small radial hole and is so located that its junction just touches the cell body. No holes are made on the cell body for the the insertion of the thermocouple since that would considerably weaken the cell body. There will be however, a difference in the temperature of the sample and that sensed by the thermocouple junction. By accurately

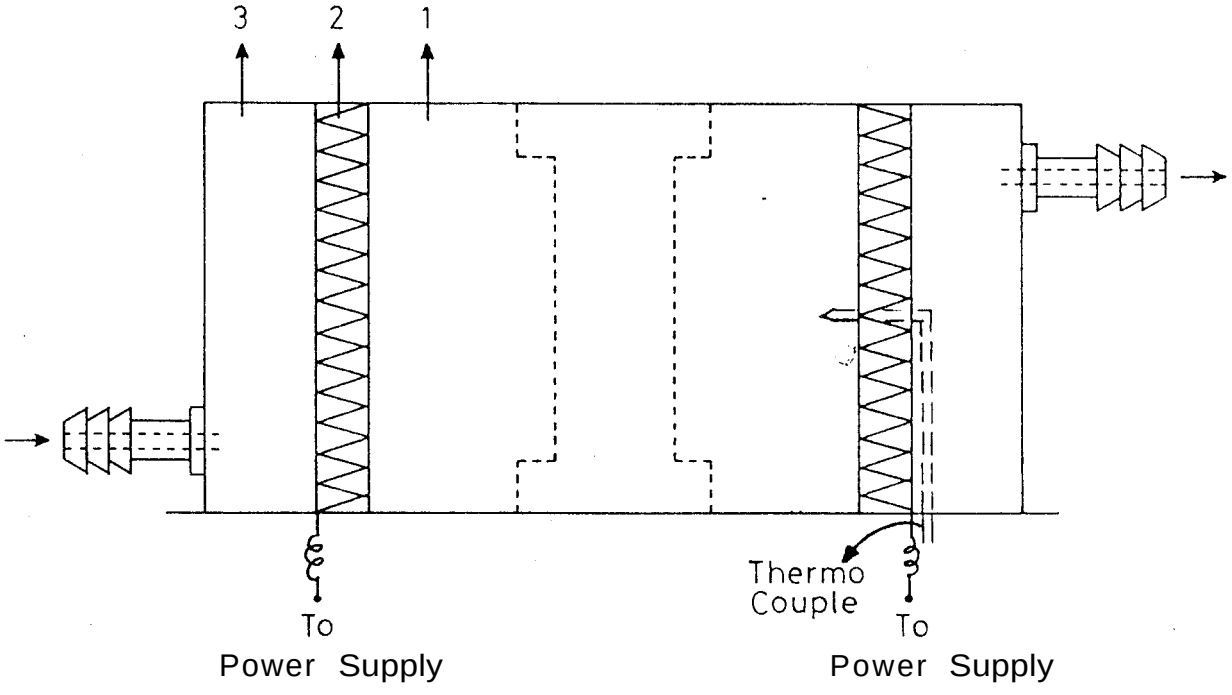

Figure 2.4 Schematic diagram of the heating and cooling assembly

1. High pressure cell
2. Heater
3. Cooling unit

mapping this gradient at all temperatures, the problem was overcome. These calibration experiments were performed using a uniform heating or cooling rate of 1°/min.

. Except in the case of lipids (Appendix), the mesophase transitions occur well above the room temperature. As such a cooling unit was necessary only when the cell had to be cooled to or below room temperature. Above room temperature cooling could be done by merely varying the current through the heating element. A cooling jacket into which the cell can be press-fitted is made using aluminimum as the material. By suitably scooping out the inside material from the jacket and by closing the top of the jacket with an aluminium strip, water can be passed into the jacket through the nozzels provided at the ends of the jacket. In fact, the jacket consisted of two 'C' shaped units linked by a hinge. So whenever cooling was necessary it could be slipped through easily. A thermostat was used to pump water into the cooling jacket. The water, as it passes through practically the entire circumference of the cooling jacket, provides a very efficient way of cooling the cell.

2.2.4 High Pressure Plumbing System

The schematic diagram of the high pressure plumbing system used in the present study is shown in fig. 2.5. A hand pump (PPI, USA) is used to generate the pressure in the cell. Fine variations of pressure are achieved by using a pressure generator (HIP, USA) with a small displacement capacity. The line pressure, which is nothing but the pressure experienced by the sample,

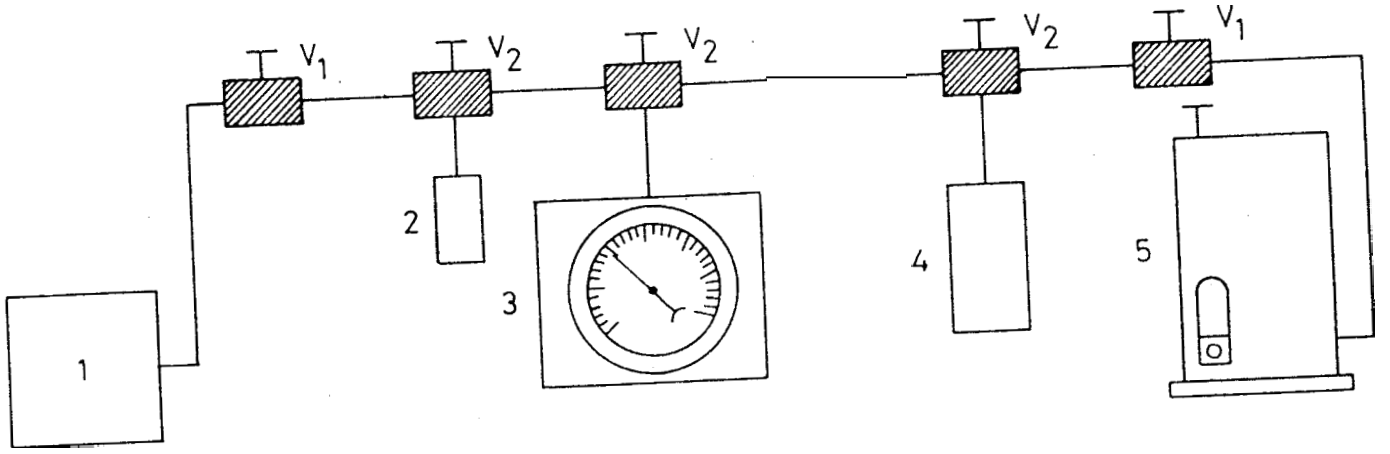

Figure 2.5 Schematic diagram of the high pressure plumbing system

1. High pressure cell
2. Pressure transducer
3. Bourdon gauge
4. Pressure generator
5. Hand pump

V_1 Two-way valve

V_2 Three-way valve

is measured by a Bourdon type (HEISE) gauge. The plumbing connections are made through two-way and three-way valves. The advantage of using a three-way valve over that of a T-joint is that the instrument which is connected through the valve can be isolated from the main line when not in use by just closing the valve. Thus for example, the pressure transducer could be used "on-line" whenever required. The tubing used was made of seamless stainless steel material (ID =2mm and OD = 10mm). The valves as well as the tubing were chosen to withstand line pressures up to 7 kbar.

The sample was pressurised in a fairly straight forward way: the "priming" was done using the hand pump. Pulling the handle of the pump up raises the piston and draws oil from the reserve into the pump's chamber. Pushing the handle down lowers the piston which compresses the oil and sends it through the steel oil line to the cell. After this priming operation pressure could be fine controlled using the pressure generator. As the pressure in the cell is the same as that in the pump the cell pressure could be indirectly measured by measuring the line pressure.

2.2.5 Determination of the Phase Transition Temperatures

The experimental set up used to determine the transition temperatures is shown in fig. 2.6. Light from a He-Ne laser (Spectra Physics 5mW) was made to fall on the sample in the optical cell. A photo detector system was positioned to collect the light transmitted by the sample. The voltage drop across a fixed resistence of 1 kilo ohms caused by the current output of the

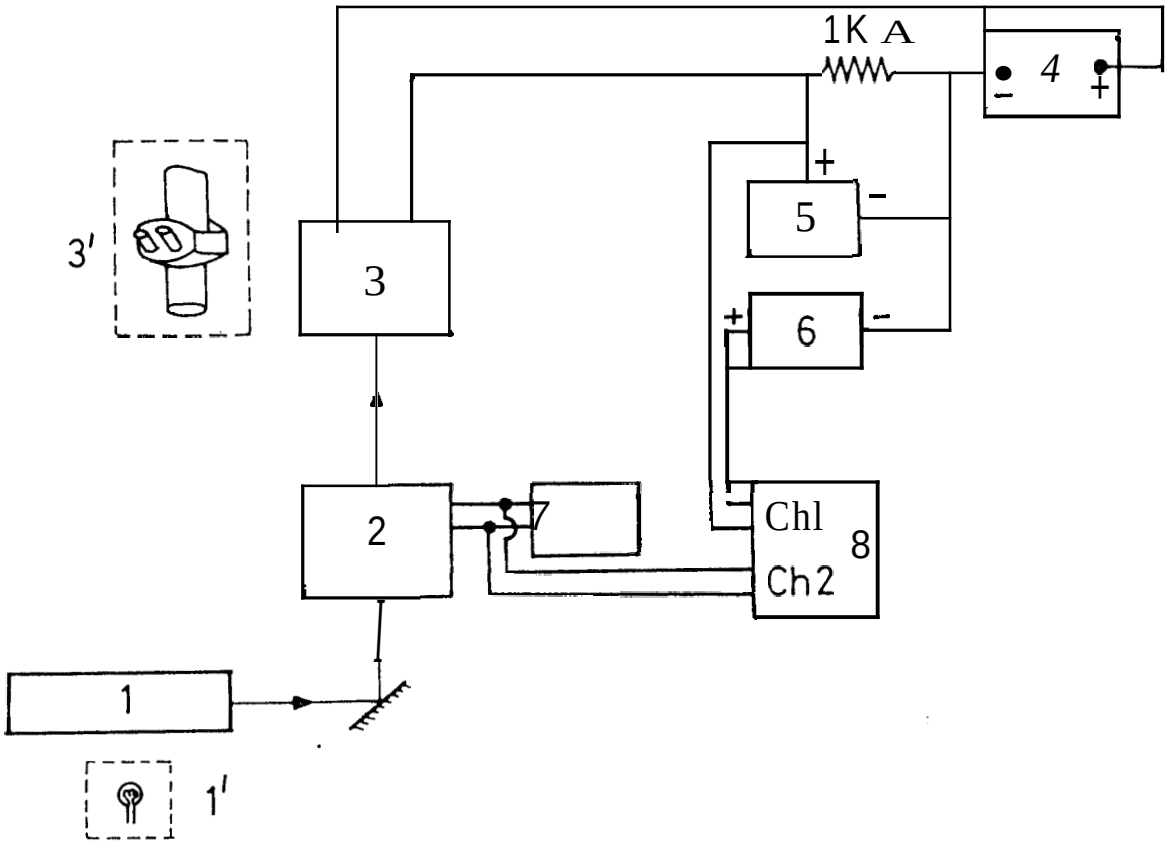

Figure 2.6 Schematic diagram of the experimental set up used for the high pressure experiments

1. He-Ne laser 2. High pressure optical cell 3. Photo detector 4. Photo detector bias power supply 5. Multimeter for measuring intensity in terms of voltage 6. DC standard source used for voltage offset 7. Multimeter for measuring the thermocouple output 8. Multichannel recorder.
Instruments indicated by primed numbers are used for microscopic observations.

detector was measured using a digital multimeter. A parallel connection from this was taken to one of the channels of a multichannel recorder (Linseis model 2041) through a low voltage source. Using the voltage source as an offset control small intensity changes over and above a large background intensity could be easily monitored. The temperature of the sample was measured using a thermocouple in conjunction with a programmable digital multimeter (Keithley 192). The voltage output of the thermocouple was fed to another channel of the multichannel recorder. Thus both intensity and temperature could be simultaneously monitored and recorded. At the phase transition there would be an abrupt change in the intensity of the transmitted light.

2.2.6 Temperature calibration of the Cell

For the temperature calibration of the cell during the heating and cooling modes, several compounds, non-mesomorphic as well as mesomorphic, have been used.

a) Heating Mode: The substances as well as their transition temperatures as measured with the polarising microscope fitted with a programmable hot stage (Mettler FP52/FP5) are listed in Table 2.1. The plot of this temperature against the transition temperatures as measured in our experimental set up is shown in fig. 2.7. The data were fitted to a straight line using a linear least square program. The values of slope and intercept thus obtained are 1.000 and 1.571°C respectively.

b) Cooling Mode: As the crystallization temperature depends on the rate

TABLE 2.1

Materials used for the temperature calibration of the high pressure cell (heating mode) and their transition temperatures

Substance	Transition	Actual Temperature(°C) (by Mettler)	Observed Temperature (°C) (by Pressure Cell)
C-CH_2	Nematic-Isotropic	48.5	51.1
Azobenzol	Solid-Isotropic	67.9	69.2
NPOOB	Nematic-Isotropic	66.2	69.5
C-CH_4	Nematic-Isotropic	79.2	80.6
Benzil	Solid-Isotropic	94.7	96.4
7 OPDOB	Solid-Smectic C	69.7	71.1
	Smectic A-Nematic	84.1	85.1
	Nematic-Isotropic	87.8	88.8
CBNA	Solid-Smectic A	72.0	73.3
	Smectic A-Nematic	99.3	100.2
	Nematic-Isotropic	105.0	106.1
HOAB	Solid-Smectic C	74.4	75.8
	Smectic C-Nematic	94.6	95.5
	Nematic-Isotropic	123.8	125.7
PAA	Solid-Nematic	118.0	119.9
	Nematic-Isotropic	135.2	137.1
PAP	Solid-Nematic	140.0	141.6
	Nematic-Isotropic	165.2	167.4

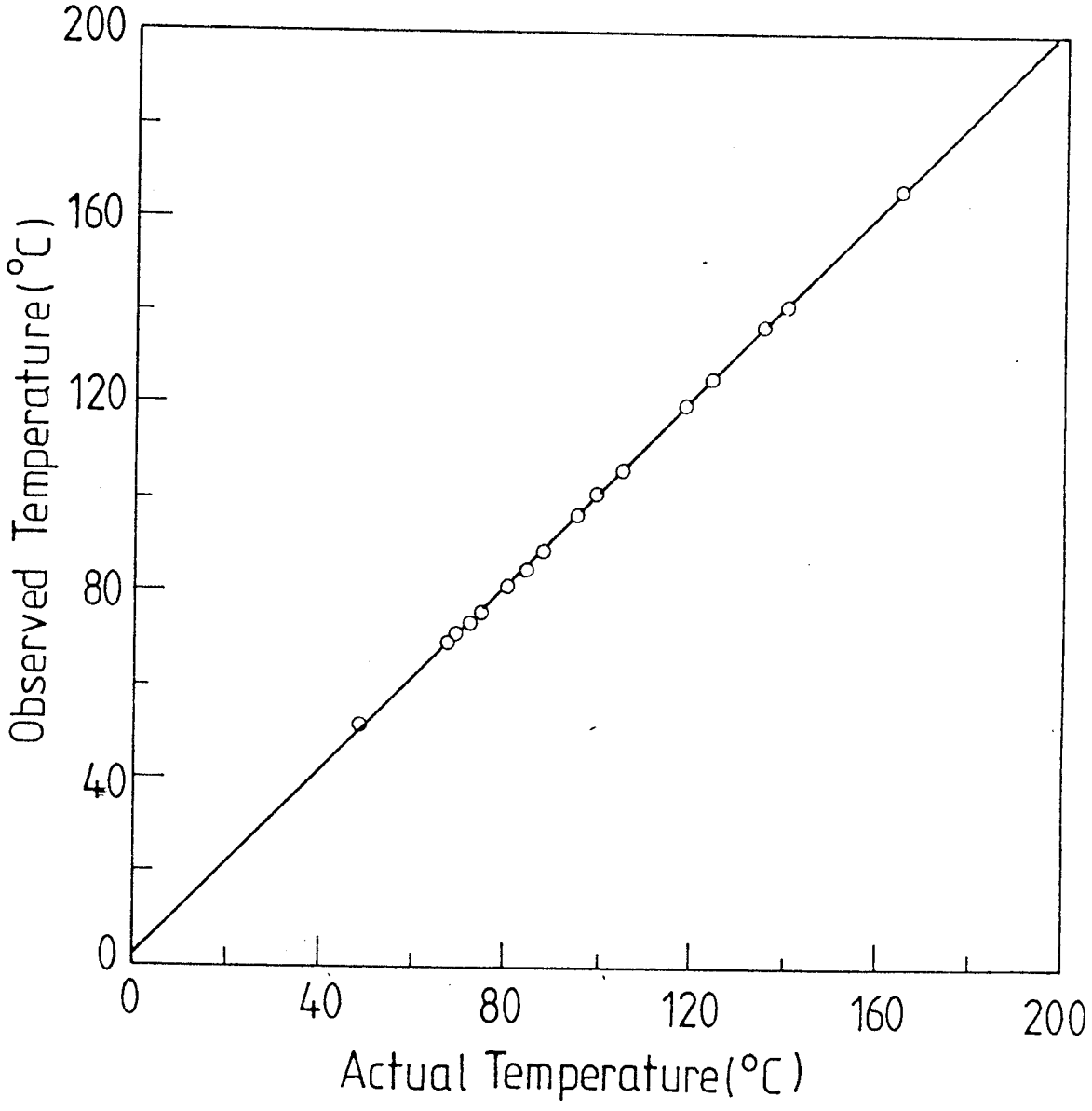

Figure 2.7 Temperature calibration curve of the high pressure cell in the heating mode using the substances listed in Table 2.1

of cooling, quantity of sample taken, etc., (i.e., the degree of supercooling is a function of the experimental conditions), the non-mesomorphic compounds cannot be used for the temperature calibration of the cell during the cooling mode. For this purpose, only liquid crystalline transitions which are highly reproducible were used in the cooling mode. The compounds used are listed in Table 2.2 along with their transition temperature as measured using the Mettler hot stage. The plot of this temprature versus the temperature measured using our set up is shown in fig. 2.8. The values of the slope and the intercept obtained by a linear least square fit of the data to a straight line are 0.985 and - 0.269°C respectively.

2.2.7 Pressure Calibration of the Cell

In order to ascertain that the pressure experienced by the sample is the same as the line pressure read on the gauge, we conducted calibration experiments using p-azoxy anisole (PAA), perhaps the most widely studied liquid crystal under pressure. The nematic-isotropic transition was used for the purpose. The experiments were conducted on both increasing and decreasing pressure cycle and it was found that the transition temperature at any pressure was independent of the pressure cycling. This showed that the sample in the cell was experiencing hydrostatic pressure.

2.3 Xray Set Up

In this section we shall describe the set up used in Xray diffraction experi-

TABLE 2.2

Temperature calibration of the high pressure cell during cooling: Materials used and their transition temperatures

Substance	Transition	Actual Temperature (°C) (by Mettler)	Observed Temperature (°C) (by Pressure Cell)
$C\text{-}CH_2$	Isotropic-Nematic	48.4	46.1
NPOOB	Isotropic-Nematic	66.2	65.8
	Nematic-Smectic A	60.1	59.3
$C\text{-}CH_4$	Isostropic-Nematic	79.0	77.8
7 OPDOB	Isotropic-Nematic	87.6	86.2
	Nematic-Smectic A	84.0	82.7
CBNA	Isotropic-Nematic	104.9	103.7
	Nematic-Smectic A	99.1	97.2
HOAB	Isotropic-Nematic	123.6	122.2
	Nematic-Smectic C	94.3	91.9
PAA	Isotropic-Nematic	135.0	132.4
PAP	Isotropic-Nematic	165.0	161.9

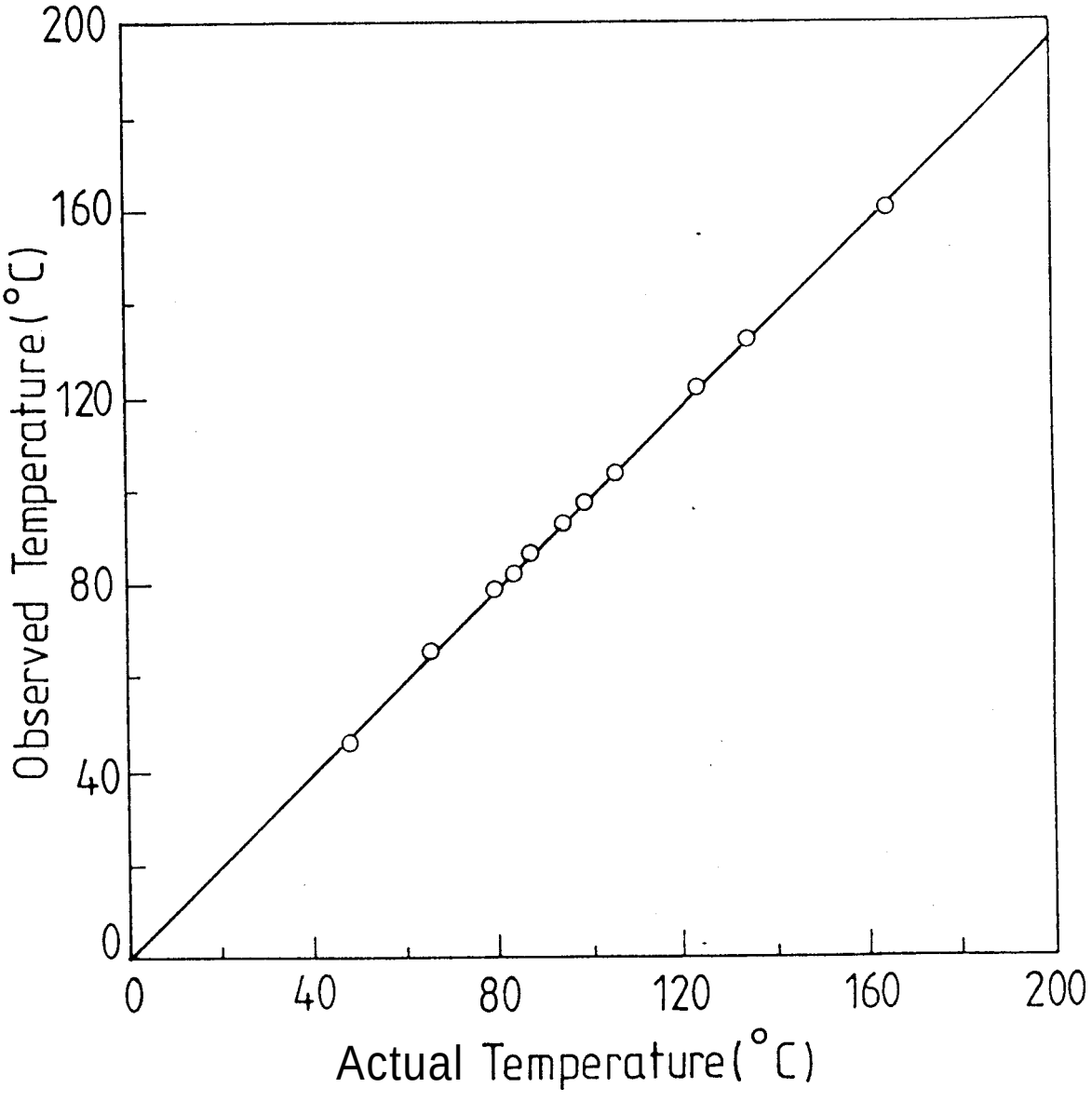

Figure 2.8 Temperature calibration curve of the high pressure cell in the cooling mode using the substances listed in Table 2.2

ments. The sample holder and the heater used to maintain the temperature of the sample at any desired value are shown in fig. 2.9. The heater consists of a circular copper rod having a rectangular slot. In order to facilitate mounting between the pole pieces of a permanent magnet, the central portion of the rod was machined to have a rectangular cross section. Nichrome tape wound on the bottom and top circular parts was used for heating the sample. A small hole (about 0.6mm diameter) was drilled at the centre of the rectangular portion for the Xrays to enter. The conical angle of the exit aperture (O_1) was about 45°.

The sample holder consisted of a long rectangular copper strip which fitted exactly into the rectangular slot of the heater. This strip had a hole (O_2) of 0.8mm diameter along the wider side through which a Lindemann capillary tube containing the sample could be inserted. The strip also had two holes (at right angles to the hole in which the sample capillary is located), one for the entrance of the Xrays and the other (O_3) for the diffracted Xray beam. The hole on the exit side had a large taper so that it permits diffraction cone angle of 45°. Both the entrance and the exit holes of the heater were covered by thin mylar strips to avoid air currents affecting the sample temperature. The heater was kept between the pole pieces of a permanent magnet of strength $\simeq$ 0.4 Tesla such that the sample position was at the centre pf the pole pieces and the field was normal to the incident Xray beam. The heater and the magnet assembly were mounted on a stand of adjustable height which also had a provision for precise leveling by means of three leveling screws.

A copper-constantan thermocouple was inserted into the heater from the bottom such that the junction was as close to the sample as possible. The output of the thermocouple was fed to a digital multimeter. Calibration of the thermocouple was done using standard samples.

For Xray studies samples were taken in Lindemann glass capillary tubes and the ends of the tubes were sealed in a flame. The tube was mounted in the sample holder and was bathed in monochromatic Cu K_α Xradiation obtained from a Xray generator (Philips W1730) in conjunction with a bent quartz crystal monochromator (Carl Zeiss Jena). The diffracted Xray beam was recorded on a flat film which was located at the focus of the monochromator. A typical exposure time was about 30 minutes. During this time the temperature of the sample could be maintained constant to within $\pm 0.1^{o}C$. After the completion of the experiment, the transition temperature of the sample was remeasured and found to be unaltered within the limits of the experimental error indicating thereby that the sample did not deteriorate during the experiment. The distance between the diffraction spots on the film was measured using a precision comparator (Adam-Hilger Ltd.,). The data thus obtained were brought to an absolute scale by using the 100 reflection of p-decanoic acid. The d value of this reflection was taken to be 23.1 A°.[6]

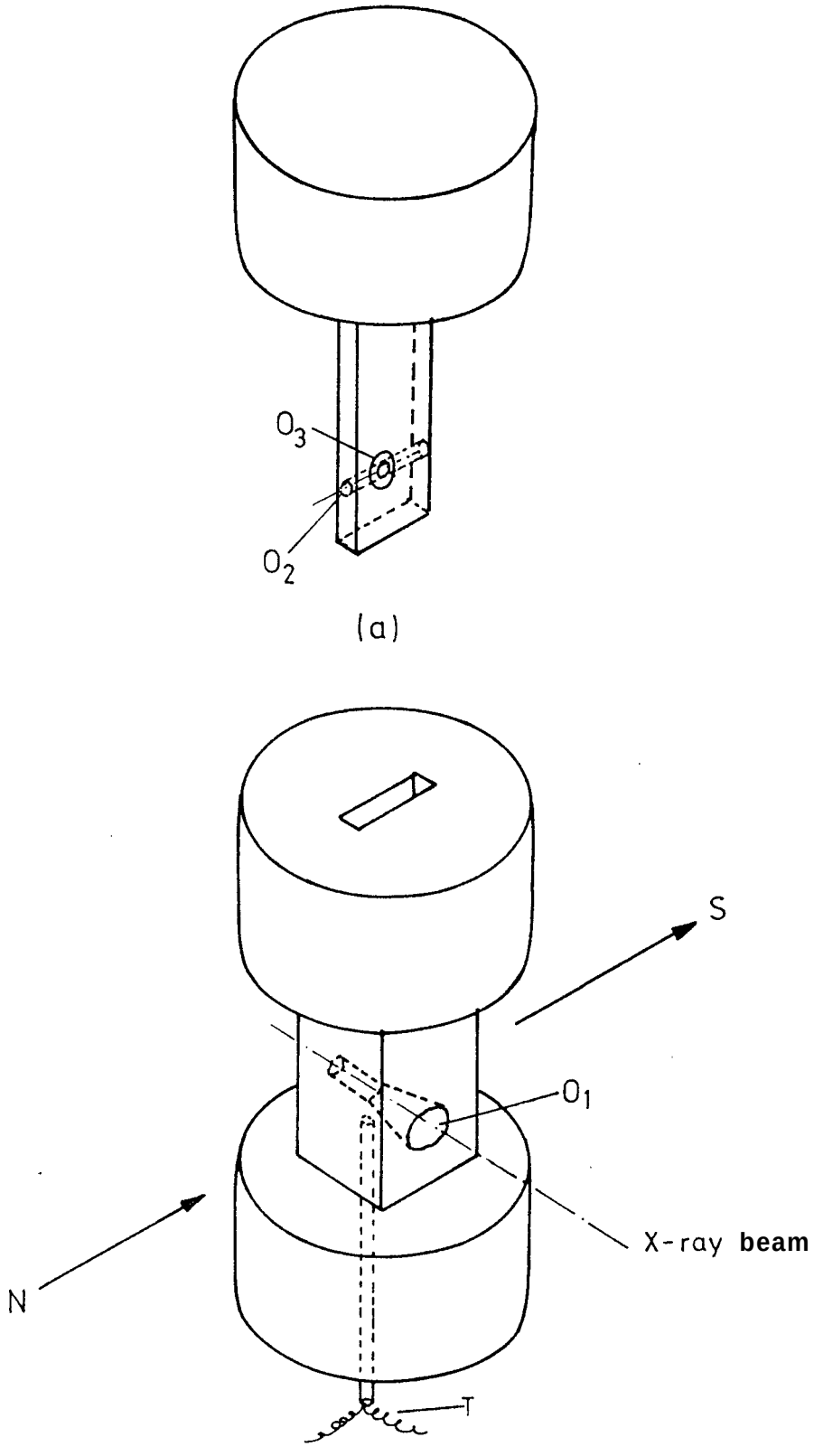

Figure 2.9 Schematic diagram of the sample holder (a) and the heater assembly (b) used for the Xray experiments

2.4 Dielectric Set Up

2.4.1 Dielectric Cell:

The dielectric constants were evaluated by measuring the capacitances of a parallel plate capacitor without and with the sample. A schematic diagram of the dielectric cell[7] is given in fig. 2.10 (a). The cell consisted of two aluminium coated glass plates which served as electrodes. These were separated by narrow strips of mylar (thickness 50 μ -100 μ). Care was taken to see that these spacers were outside the active area which was about 0.8 cm^2. A bevel made on the shorter side of one of the plates was useful in filling the sample. The plates were offset along the length and the area jetting out was used to make electrical contacts. The electrode assembly was held rigidly in a copper frame shaped like a rectangular G clamp. A flat copper plate was used as a buffer to avoid uneven pressing of the plates by the brass screws.

2.4.2 Heater for the Dielectric Cell

A schematic diagram of the heater is shown in fig. 2.10 (b). The heater consisted of a copper rod having a rectangular slot along its length. A thin sheet of mica was stuck over the surface of the tube so that nichrome tape could be wound over it. Asbestos sheet covering on the outside provided good thermal insulation. The heater, could be rotated about a vertical axis and its position could be read on a circular scale attached to its bottom to a precision of 0.1°C. With this attachment the cell could be rotated exactly by 90°C facilitating a quick switchover from $\varepsilon_\perp$ measuring configura-

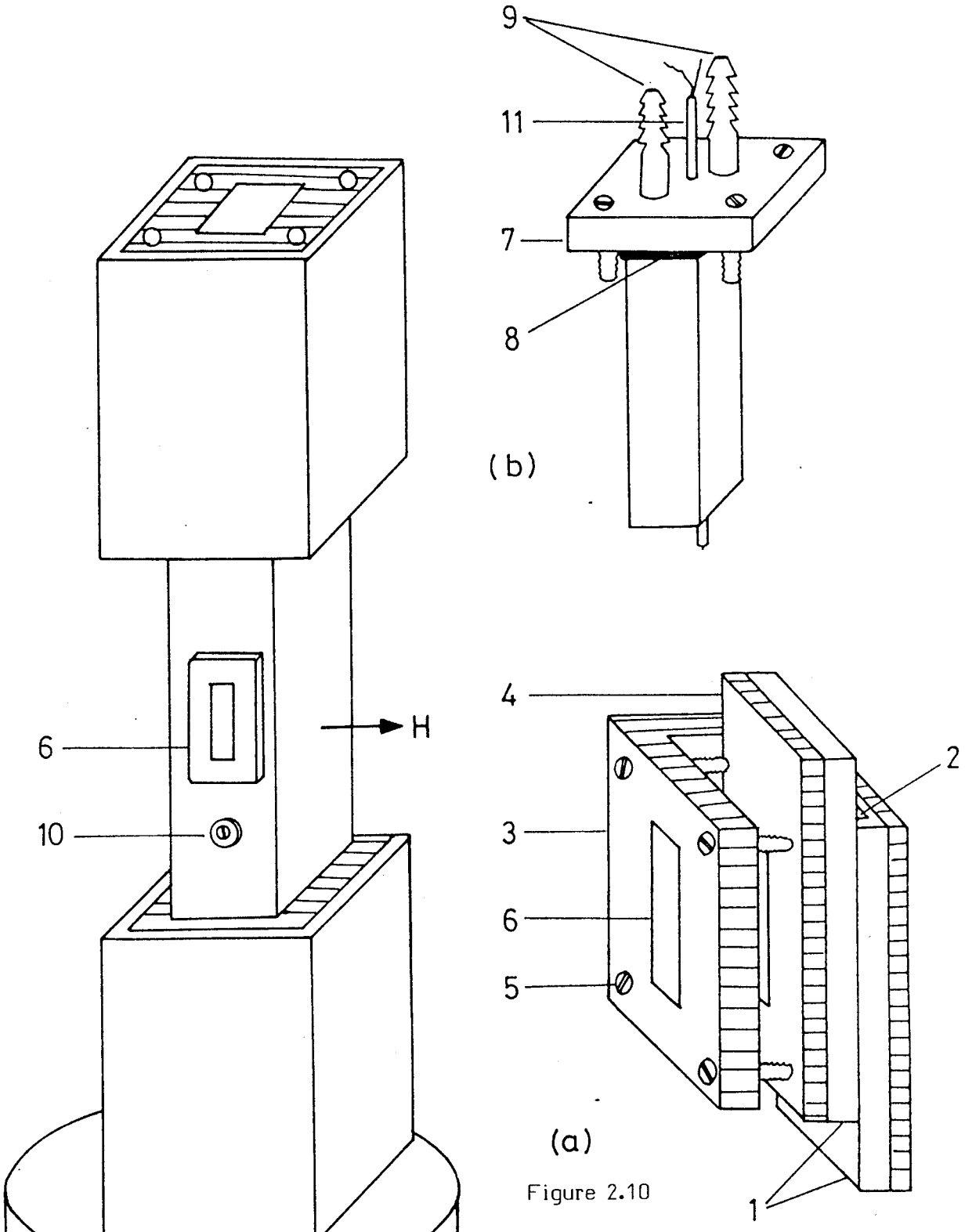

Figure 2.10

Schematic diagram of the (a) dielectric cell (b) heater

1. Electrodes
2. Bevel
3. Copper clamp
4. Copper plate
5. Brass screws
6. Windows
7. Copper cap
8. Neoprene gasket
9. Nozzels
10. Brass nuts
11. Thermocouple

tion to $\varepsilon_{\parallel}$ measuring configuration and vice versa. The heater was sealed by a neoprene gasket in the copper cap which in turn could be screwed on to the top of heater. Before the commencement of any experiment the heater was flushed with dry nitrogen for a long time through a pair of nozzles in order to prevent oxidation and hence deterioration of the sample. The heater assembly was mounted on a stand between the pole pieces of a water cooled magnet (Field - 1.5 Tesla). The field was more than the saturation field required to orient the sample (thickness 50μ-100μ).

The temperature of the sample was measured using a calibrated Chromel-Alumel thermocouple in conjunction with a digital multimeter. Temperature of the sample was maintained constant to ±25mK during the dispersion studies. For the static measurements a slow rate of cooling (about 6°C/hr) was adapted.

For the measurement of $\varepsilon_{\parallel}$ (dielectric constant along the director), the sample was aligned homeotropically and the electric firld was applied along the director. $\varepsilon_{\perp}$ was measured by aligning the sample homogeneously and applying the electric field perpendicular to the director.

The static dielectric measurement as well as dispersion studies were performed using a Hewlelt Packard Impedance analyser (4192A) whose frequency range is 5Hz - 13MHz.

As the alignment was produced by a strong magnetic field and not by means of surface treatment or surfactants, it is reasonable to assume that the surface anchoring effect was negligibly small. In such a case the entire sample would be aligned with the director along the magnetic field, and hence the relative accuracy in the measurement of $\varepsilon_{\parallel}$ and $\varepsilon_{\perp}$ would be the same as that for the capicatance measurement which in our case is 0.1%. In the extreme, but unlikely possibility of strong surface anchoring which conflicts the direction of the magnetic field, there would be a boundary layer (or a magnetic coherence length as defined by de Gennes[8]) whose thickness is a function of temperature because of the thermal dependence of the elastic constants. This would of course affect the dielectrir constant measurements and the error would be much greater. However, as remarked earlier such a situation is very unlikely.

The precision in the determination of the frequency of relaxation and hence the activation energy is estimated to be 2%.

References

1. S.Chandrasekhar and R.Shashidhar, "Advances in Liquid Crystals",Vol.4, Ed. G.H.Brown (Academic Press, 1979) p.83.

2. G.A.Hulett, Z. Phys. Chem., 28, 629 (1899); J.Robberecht, Bull. Soc. Chim. Belg., **47**, 597 (1938).

3. P.H.Keyes, H.T.Weston and W.B.Daniels, Phys. Rev. Lett., 31, 628 (1973).

4. P.E.Cladis, R.K.Bogardus, W.B.Daniels and G.N.Taylor, Phys. Rev. Lett., 39, 720 (1977).

5. A.N.Kalkura, R.Shashidhar and M.Subramanya Raj Urs, J.Physique, 44, 51 (1983); A.N.Kalkura, "High Pressure Optical Studies of Liquid Crystals", Ph.D. Thesis, University of Mysore, 1982.

6. P.E.Cladis and D.Guillon (Private Communication).

7. For a detailed description see B.R.Ratna, "Dielectric Properties and Short Range Order in Liquid Crytstals", Ph.D. Thesis, University of Mysore, 1978.

8. P.G.de Gennes, Mol. cryst. Liq. Cryst., 12, 193 (1971); see also P.G.de Gennes, "The Physics of Liquid Crystals", Clarendon Press, Oxford (1974).